Dianiline Schiff Bases as Inhibitors of Mild Steel Corrosion in Acid Media

S. Chitra[1,], K. Parameswari[1], A. Selvaraj[2]*

[1] Department of Chemistry, P.S.G.R.Krishnammal College for Women, Coimbatore, Tamilnadu, India,
[2] Department of Chemistry, CBM College Coimbatore, Tamilnadu, India
[*]E-mail: rajshree_shree1995@yahoo.com

A new class of corrosion inhibitors namely dianiline Schiff bases was synthesized and its inhibiting action on the corrosion of mild steel in 1M sulphuric acid at 30°C was investigated by various corrosion monitoring techniques. A preliminary screening of the inhibition efficiency was carried out using weight loss measurements. Potentiodynamic polarization studies showed that the Schiff bases were mixed type inhibitors. The effect of temperature on the corrosion behaviour of mild steel in 1M sulphuric acid with the addition of the Schiff bases was studied in the temperature range from 40°C-60°C. The adsorption of these compounds on a mild steel surface from sulphuric acid obeyed the Langmuir adsorption isotherm. The decrease in inhibition efficiency with increase in temperature and the less negative $\Delta G°_{ads}$ values suggest predominant physisorption of the Schiff base molecules on the steel surface.

1. INTRODUCTION

One of the most vital processes in the field of prevention of corrosion and its control is the use of organic inhibitors. The crucial part in the mechanistic aspect of such inhibitors is the specific interaction between certain functionalities in the inhibitors with the corrosion active centres on the metal surface. Heteroatoms such as nitrogen, oxygen, sulphur present in the inhibitors play a leading role in this interaction by donating their free electron pairs [1-10]. Hence most of the organic compounds containing these heteroatoms generally act as good inhibitors. In addition, compounds with multiple bonds behave as efficient inhibitors due to the availability of π-electrons for interaction with the metal surface. Certain inhibitors possess both the above two features, *viz.,* availability of lone pair

from heteroatom as well as π-electrons in the same molecule, and such compounds show extraordinary inhibition characteristics. Schiff bases are the best known examples of this category and have been investigated for the inhibition of acid corrosion of mild steel [11,12], aluminium [13] and copper[14], and for the neutral halide corrosion of copper [15-17].

Table 1. Structure of the Schiff bases

Name	Structure of the Schiff bases
DAA	 N,N′-Bis(benzylidene)-4,4'-dianiline
MDAA	 N,N′-Bis(benzylidene)-4-4′-methylenedianiline
SDAA	 N,N′-Bis(benzylidene)-4-4′-sulphonyldianiline
ODAA	 N,N′-Bis(benzylidene)-4-4′-oxydianline
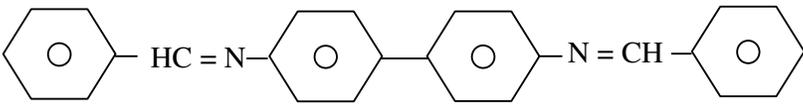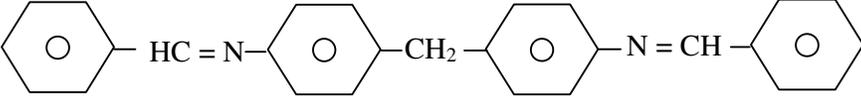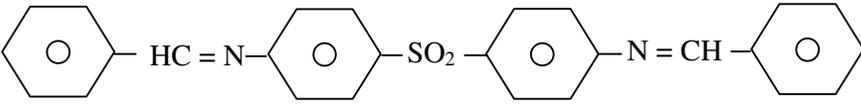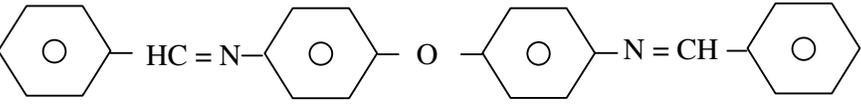
Schiff bases are the condensation products of carbonyls and amines and are also called anils. Although most of the commercial formulations of inhibitors include aldehydes and amines as essential ingredients [18,19], Schiff bases have been found to possess more inhibition efficiency than their constituent carbonyls and amines [20-23]. Certain authors have attributed this considerably stronger inhibition efficiencies to the presence of unoccupied π*-orbitals in the Schiff base molecules, which enable electron back donation from the transition metal d-orbitals and thereby stabilise the existing metal-inhibitor bond, which is not possible with the constituent amines[24].

The review of literature reveals that despite the superlative inhibition characteristics of Schiff bases in general, this class of compounds has not been so far exploited to the extent of their high potential. Further the influence of wide range of structural variation on their inhibition efficiencies has not also been thoroughly investigated. Hence it has been thought fit to synthesise a series of Schiff bases by condensing benzaldehyde with dianilines and to study the inhibitive performance for the

corrosion of mild steel in acid medium. Sulphuric acid and hydrochloric acid are commonly used for various industrial applications such as acid pickling, descaling, in oil wells etc. Hence, the effect of dianiline Schiff bases on the corrosion rate, corrosion potential, anodic and cathodic polarization behaviour of steel in 1M sulphuric acid has been investigated as it is the most commonly used electrolyte in industries for acid pickling, surface cleaning, acidizing etc. The structures of the newly synthesized dianiline Schiff bases are given in table 1.

2. EXPERIMENTAL DETAILS

A range of techniques were used for the evaluation of inhibition efficiency.

2.1. Non-electrochemical measurements

2.1.1. Weight loss technique

The experiments were performed on steel with the following chemical composition iron-99.099% and carbon-0.084%. Gravimetric measurements were carried out in a double walled glass cell equipped with a thermo stated cooling condenser. The solution volume was 200ml. Rectangular steel specimens of size 5 cm × 2 cm × 0.05 cm cut from commercial mild steel sheet stock (0.05 cm thick) were used. Prior to immersion the steel specimens were polished with 4/0, 3/0, 2/0 and 1/0 grade emery papers, washed thoroughly with doubly distilled water, degreased with acetone and finally dried in air.

The initial weight of the polished specimens were measured. The test solution (200 ml) was taken in a 250 ml beaker and the mild steel specimens with a hole (0.5 cm diameter) in triplicate were suspended in the solution using glass hooks. Care was taken to ensure the complete immersion of the specimen. The temperature was maintained constant throughout the experiment at 30±1°C. After a period of 3 hours the specimens were removed, washed with running water, dried and weighed to the accuracy of four decimal places. From the initial and final weight (ie before and after immersion in solution) the loss in weight of each specimen due to corrosion was calculated. The experiment was repeated for various concentrations of the inhibitors, DAA, SDAA, MDAA and ODAA in 1M sulphuric acid. To determine the effect of temperature the above procedure was carried out in the temperature range 40°C-60°C.

From the weight loss measurements, the percentage inhibition efficiency, corrosion rate and surface coverage was calculated for the various inhibitor concentrations using the following formulae..

$$\text{Inhibition efficiency} \, (\%) = \frac{\text{Weight loss without inhibitor - Weight loss with inhibitor}}{\text{Weight loss without inhibitor}} \times 100$$

$$\text{Corrosion rate (mpy)} = \frac{534 \times \text{Weight loss in mgm}}{\text{Density (g/cc)} \times \text{Area (Sq. inch)} \times \text{Time (hrs)}}$$

$$\text{Surface coverage} = \frac{[\text{Weight loss without inhibitor - weight loss with inhibitor}]}{\text{Weight loss without inhibitor}}$$

The activation energy (E_a) was calculated by graphical method by plotting log corrosion rate vs 1000/T K for the temperatures 30°C, 40°C, 50°C and 60°C in 1M sulphuric acid with and without inhibitor at a concentration of 10mM.

$E_a = 2.303 \times 8.314 \times \text{slope}$

The free energy of adsorption was calculated from the equilibrium constant of adsorption using the equation[23].

$\Delta G°_{ads} = - RT \ln (55.5K)$

where, $K = \theta/c(1-\theta)$ (from Langmuir equation)

θ = Surface coverage of the inhibitor

C = Concentration of the inhibitor in mM/200ml

2.1.2. Gasometric technique

Mild steel specimens of size 5 cm × 2 cm × 0.05 cm were polished to a fine mechanical finish and degreased with trichloroethylene. The specimens were stored in a desiccator. The specimen was suspended from the hook of the glass stopper and was introduced into the cell containing 200 ml of 1M sulphuric acid. The temperature was maintained constant throughout the experiment at 303±1°K and at constant atmospheric pressure. The hydrogen gas was collected over a dilute solution of sodium chloride (as hydrogen has negligible solubility in sodium chloride solution) coloured by methyl red in a gas collector for a duration of an hour.

Experiments were repeated under identical conditions for inhibitor solution of different concentrations. From the volume of hydrogen gas liberated the inhibition efficiency was calculated using the formula,

$$\text{Inhibition efficiency (\%)} = \frac{V_B - V_I}{V_B} \times 100$$

Where,

V_B -The volume of hydrogen evolved in the absence of inhibitor and

V_I-The volume of hydrogen evolved in the presence of inhibitor

2.2. Electrochemical techniques

Electrochemical techniques are now widely used to study the efficiency of the inhibitors. Since the electrochemical corrosion is the result of current flow between anodic and cathodic areas on a metal surface, the effect of the inhibitor will be to reduce this current.

The electrodes used for the electrochemical studies were made from a cylindrical mild steel rod of the same composition used for the weight loss tests. They were embedded in Teflon with an exposed area of 0.785 cm^2. The exposed area of steel was polished using 1/0, 2/0,3/0 and 4/0 emery papers, degreased with trichloroethylene and immediately used for the experiment.

The electrochemical measurements were carried out in a glass cell with a capacity of 100 ml. A platinum electrode was used as counter electrode and a saturated calomel electrode (SCE) as the reference electrode along with a Luggin capillary. The mild steel electrode was then placed in the test solution for 10-15 minutes before testing commenced.

2.2.1. Electrochemical impedance spectroscopy (EIS)

Impedance measurements were carried out at the open circuit potential using a computer controlled Solartron Model 1280B potentiostat. After immersion of the specimen, prior to the impedance measurement, 30 minutes was allowed for E_{corr} to attain a stable value before the tests were commenced. The ac frequency range extended from 10 kHz to 0.01 Hz with a signal amplitude of 10 mV at the corrosion potential. The measurements were automatically controlled by Z-view software and the impedance diagrams are given in the Nyquist representation (Z_{real} vs $Z_{imaginery}$). From the Nyquist plots electrochemical parameters, double layer capacitance (C_{dl}) and charge transfer assistance (R_t) were calculated. The inhibition efficiency was calculated using the relation.

$$\text{Inhibition efficiency } (\%) = \frac{R_t(inh) - R_t(blank)}{R_t(inh)} X 100$$

Where,

$R_{t\ (inh)}$ is the charge transfer resistance in the presence of inhibitor and

$R_{t\ (blank)}$ is the charge transfer resistance in the absence of inhibitor.

2.2.2. Polarisation measurements

The Tafel polarization measurements were made after EIS studies in the same cell setup, for a potential range of -200 mV to +200 mV with respect to open circuit potential, at a scan rate of 1

mV/sec. From the plot of E vs Log i, the corrosion potential E_{corr}, corrosion current I_{corr}, Tafel slopes b_a and b_c were obtained in the absence and in the presence of inhibitors at various concentrations.

$$\text{Inhibition efficiency (\%)} = \frac{I_{corr}(blank) - I_{corr}(inh)}{I_{corr}(blank)} X100$$

Where,

I_{corr} (blank) is the corrosion current in the absence of inhibitor and

I_{corr} (inh) is the corrosion current in the presence of inhibitor.

2.3. Surface examination and analysis of corrosion products

2.3.1. Scanning Electron Microscope (SEM)

The Joel Scanning Electron Microscope (SEM) was used to understand the surface morphology of the mild steel specimen in 1M sulphuric acid in the presence and absence of inhibitors.

2.3.2. UV-reflectance spectral studies

The inhibition of corrosion of mild steel in acidic solutions in the presence of organic compounds may be due to the formation of a film on the metal surface. The presence of such a film was studied using a reflectance UV spectrophotometer. UV-reflectance spectra in the range 200-700 nm at a normal incident angle (90°) using UV visible NIR spectrophotometer were obtained for polished steel specimens and for specimens exposed to the acid environment with and without the inhibitors (DAA, SDAA, MDAA and ODAA).

2.3.3. Analysis of corrosion products

a. Mild steel specimens of size 5 cm × 2 cm × 0.05 cm, after finely polishing with emery sheets of 1/0, 2/0, 3/0 and 4/0 grades, were degreased with trichloroethylene and immersed in 1M sulphuric acid solution with and without inhibitors (DAA, SDAA, MDAA and ODAA). After three hours of exposure to the corrosive solutions, the specimens were removed washed and the corrosion products were scraped off using glass knife and stored in a desiccator.

b. The sample for FT IR studies were prepared by finely mixing the corrosion products with spectroscopically pure KBr and pressed by using a die so as to get a fine transparent specimen and the spectrum was recorded.

Table 2. Inhibition efficiency of the inhibitors in 1M sulphuric acid at $30 \pm 1°C$

Compound name	Inhibitor concentration (mM)	Weight loss in gm	Inhibition efficiency (%)	Corrosion rate (mpy)	Degree of surface coverage (θ)
SDAA	Blank	0.6361	-	9709.74	-
	0.5	0.0744	88.28	1132.62	0.8828
	2	0.042	93.39	641.1	0.9339
	5	0.0291	95.42	444.19	0.9542
	7.5	0.0256	95.97	390.77	0.9597
	10	0.0207	96.73	315.97	0.9673
MDAA	Blank	0.9210	-	14058.6	-
	0.5	0.1670	81.86	2549.17	0.8186
	2	0.0420	95.43	641.1	0.9543
	5	0.0180	98.04	274.76	0.9804
	7.5	0.011	98.75	167.90	0.9875
	10	0.009	99.02	137.38	0.9902
DAA	Blank	0.6361	-	9709.74	-
	0.5	0.0952	85.03	1453.18	0.8503
	2	0.0258	95.94	393.82	0.9594
	5	0.0092	98.54	140.43	0.9854
	7.5	0.0067	98.94	102.27	0.9894
	10	0.0048	99.23	73.26	0.9923
ODAA	Blank	0.6361	-	9709.74	-
	0.5	0.0878	86.20	1340.2	0.8620
	2	0.0738	88.40	1126.5	0.8840
	5	0.0616	90.32	940.3	0.9032
	7.5	0.0502	92.11	766.27	0.9211
	10	0.0482	92.42	735.75	0.9242

After weight loss experiments a sample of the corrodent solution was taken out, diluted with distilled water and analyzed for the concentration of iron using atomic absorption spectrophotometer. The corrodant solution was treated with dithiozone reagent. The red coloured chelate was extracted with ammonium pyrrolidine dithiocarbamate into methyl isobutyl ketone. This organic extract was directly fed into an air-acetylene flame of an atomic absorption spectrophotometer and its absorbance of recorded at 248.3 nm. A standard curve was prepared under identical conditions.

Table 3. Inhibition efficiency of the inhibitors at higher temperature in 1M sulphuric acid (concentration of inhibitor = 10 mM)

Compound name	Temperature	Weight loss in gm	Inhibition efficiency (%)	Corrosion rate (mpy)	Degree of surface coverage (θ)
SDAA	303 K	0.0069	96.73	315.97	0.967
	313 K	0.0239	90.57	1096.4	0.9057
	323 K	0.033	87.77	1513.5	0.8777
	333 K	0.0456	84.69	2089.3	0.8469
MDAA	303 K	0.003	99.02	137.8	0.9902
	313 K	0.0251	90.09	1149.3	0.9009
	323 K	0.069	83.27	3162.27	0.8327
	333 K	0.1582	79.91	7244.35	0.7991
DAA	303 K	0.0016	99.23	73.26	0.9923
	313 K	0.0975	86.7	4464.52	0.867
	323 K	0.199	72.89	9112.21	0.7289
	333 K	0.338	67.28	15477.12	0.6728
ODAA	303 K	0016	92.42	735.75	0.9242
	313 K	0.0240	90.68	1099.4	0.9068
	323 K	0.0587	85.67	2687.87	0.8567
	333 K	0.158	70.76	7392.82	0.7076

3. RESULTS

3.1. Weight loss method

The average weight loss data obtained for the mild steel specimen in triplicates for various concentrations of inhibitors (DAA, MDAA, SDAA and ODAA) are presented in table 2. From the weight loss data which were obtained by performing the experiment in triplicate with the data variation of 0.5 mg, it is clear that the loss in weight of mild steel specimens decreases with increasing inhibitor concentration. Hence for the four inhibitors the inhibition efficiency (IE) increases with the increase in concentration. The IE results from table 2 are depicted in figure 1 (IE vs inhibitor concentration).
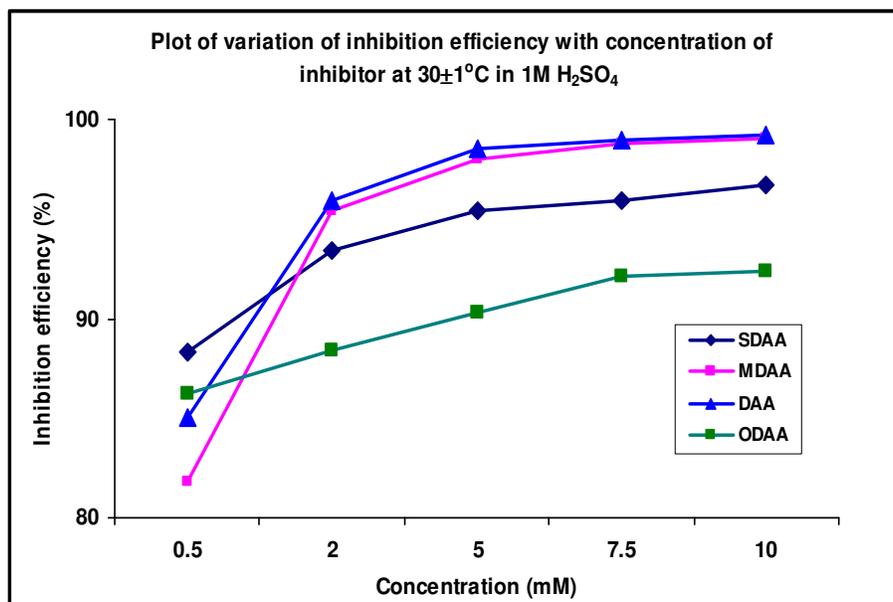
Figure 1. Plot of variation of inhibition efficiency with concentration of inhibitor at 30 ± 1^0C in $1MH_2SO_4$

Maximum inhibition efficiency (99 %) was observed for DAA and MDAA. The degree of surface coverage (θ) for different concentrations of inhibitors has been evaluated from weight loss method. The data were plotted using the Langmuir isotherm with Log $\theta/1-\theta$ vs Log C for all the compounds (figure 2) A straight line was obtained in all the cases indicating that the adsorption of these compounds on the mild steel surface obeys Langmuir adsorption isotherm.

To investigate the mechanism of inhibition and to calculate the thermodynamic parameters of the corrosion process, weight loss measurements were taken at various temperatures (313 -333 °K) at 10 mM concentration of the inhibitor. The effect of temperature on the corrosion inhibition of mild steel in 1M sulphuric acid with and without various inhibitors are given in table 3. It was found that the weight loss increased linearly with the increase of temperature in the absence and in the presence of inhibitors.
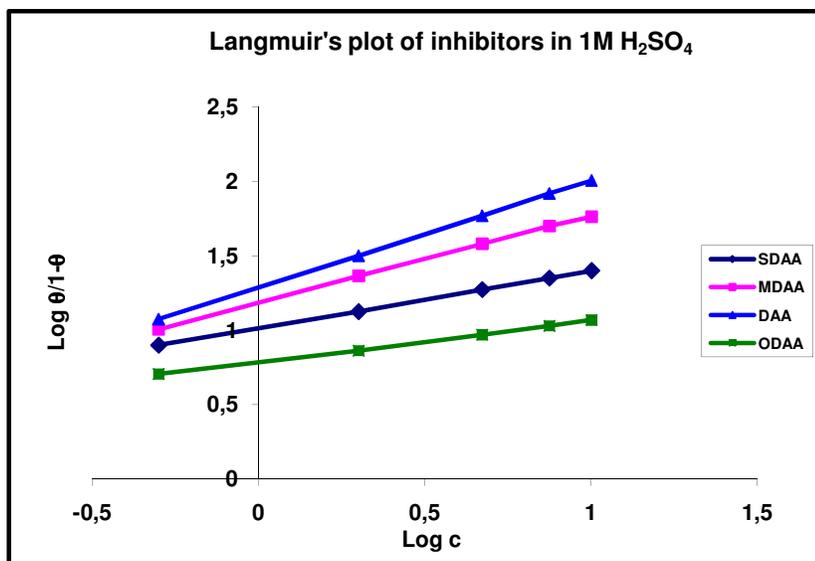
Figure 2. Langmuir's plot of inhibitors in 1M H_2SO_4

The activation energies for the corrosion process were estimated from the slopes of the lines of the Arrhenius plots (figure 3) and are given in table 4. The values of E_a for the inhibited systems were higher than those of the uninhibited systems.

Table 4. Activation energies (E_a) and free energies of adsorption ($\Delta G°_{ads}$) for the corrosion of mild steel in 1M sulphuric acid at selected concentrations of the inhibitors

Name of the inhibitor	E_a (kJ)	$\Delta G°_{ads}$ at various temperatures (kJ)			
		303 K	313 K	323 K	333 K
Blank	38.29	-	-	-	-
SDAA	41.59	-12.89	-15.01	-9.89	-9.52
MDAA	76.58	-15.94	-10.203	-8.912	-8.569
DAA	85.09	-16.16	-11.27	-9.40	-7.19
ODAA	41.02	-11.63	-9.33	-7.25	-6.74

3.2. Gasometry

The inhibitor efficiency was also determined for the dianiline Schiff bases using gasometric method from the volume of gas collected in the absence and presence of inhibitors at 30±1°C for the corrosion of mild steel in 1M sulphuric acid. The volume of gas collected decreased with the addition of inhibitors (table 5). The rate of cathodic hydrogen evolution reaction due to the increased level of inhibition leads to the decrease in the volume of hydrogen gas evolved suggesting that the inhibitor efficiency increases with increase in the concentration of the inhibitors similar to weight loss method.

Table 5. Gasometric method Inhibition efficiency of the inhibitors in 1M sulphuric acid at 30±1°C

Compound name	Inhibitor concentration (mM)	Volume of gas (cc)	Inhibition efficiency (%)
SDAA	Blank	36.5	-
	0.5	7.8	78.63
	7.5	2.3	93.69
	10	1.2	96.71
MDAA	Blank	41.4	-
	0.5	9.1	78.01
	7.5	1.3	96.85
	10	0.9	97.82
DAA	Blank	41.4	-
	0.5	7.3	82.36
	7.5	1.7	95.89
	10	0.5	98.79
ODAA	Blank	41.4	-
	0.5	7.9	81.15
	7.5	4.7	88.64
	10	4.2	89.85

3.3. Impedance spectroscopy

Impedance spectroscopic studies were made for mild steel in 1M sulphuric acid at 30 ±1°C at various concentrations of the four inhibitors SDAA, MDAA, DAA, ODAA and the Nyquist plots were constructed. These plots are presented in figure 4. From these plots the charge transfer resistance R_t values were determined from the differences in impedance at low frequency and high frequency as

proposed by Haruyama[25]. The determination of charge transfer resistance R_t and double layer capacitance C_{dl} is based on the concept of equivalent circuit given below.
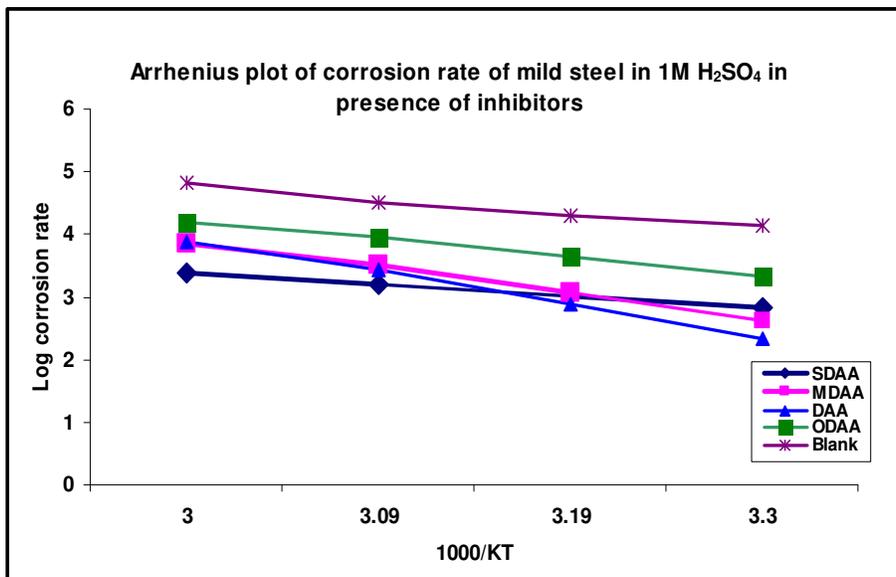
Figure 3. Arrhenius plot of corrosion rate of mild steel in 1M H_2SO_4 in presence of inhibitors

A simple electrode reaction such as metal deposition or metal dissolution can be represented by an equivalent circuit, named as Randles equivalent circuit with various components according to

C_{dl} = Double layer capacitance
R_Ω = Series resistance
R_t = Charge transfer resistance
W = Warburg impedance
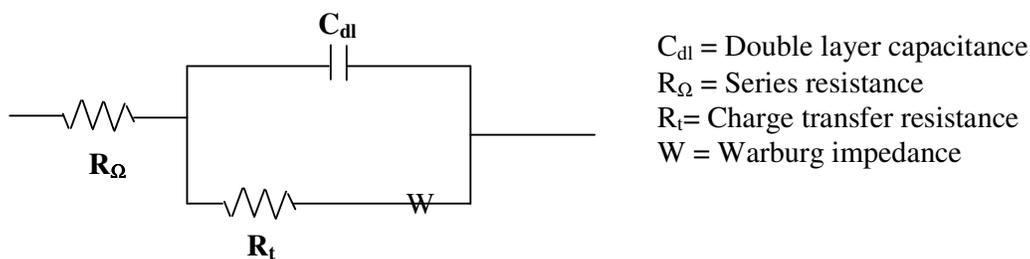
Scheme 1. Equivalent circuit of electrode impedance

This circuit represents the cell impedance under the most simplified circumstances, with which the various components of the cell have been derived by Randles[26], Delahay[27] and Sluyters *et al* [28].

In the case of an irreversible electrode process such as corrosion and at high frequencies, the process is activation polarization controlled. The concentration polarization, σ can be neglected and the equivalent circuit to a great approximation is modified as in figure.
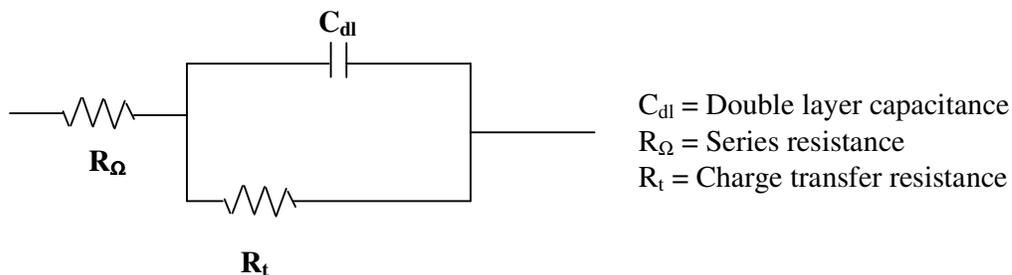
Scheme 2. Modified equivalent circuit of electrode impedance

Consequently the real and imaginary components of cell impedance becomes

$$Z' = R_\Omega + R_t / \left(1 + w^2 C_{dl}^2 R_t^2\right) \qquad (1)$$

$$Z'' = w C_{dl} R_t^2 / \left(1 + w^2 C_{dl}^2 R_t^2\right) \qquad (2)$$

Elimination of ω is performed by inserting

$$w = Z'' / (Z' - R_\Omega) R_t C_{dl}$$

into (1) and rearranging to

$$\left[Z' - R_\Omega - \frac{R_t^2}{2}\right] + \left[Z''\right]^2 = \frac{R_t^2}{4} \qquad (3)$$

which is the equation of a semicircle (Z'' vs Z' - constant concentration) with its centre on the Z' axis at $Z' = R_\Omega + 1/2\, R_t$ and radius $1/2\, R_t$. The interaction with the Z' axis are at $Z' = R_\Omega$ for $w = \infty$ and at $Z' = R_\Omega + R_t$ for $w = 0$. These are called Nyquist plots.

The charge transfer resistance values derived for different inhibitor concentrations are presented in table 6. The charge transfer resistance values were found to increase with increase in inhibitor concentration.

The double layer capacitance C_{dl} values for different inhibitor concentrations have been derived using the relation.

$$C_{dl} = \frac{1}{2\pi f_{max} R_t}$$

In the above relation f_{max} is the frequency at which the imaginary component of the impedance *viz.*, Z'' is maximum. R_t increases with increase in inhibitor concentration. Increase in R_t indicates the retordation of corrosion reaction both at anodic and cathodic sites. The decrease in double layer capacitance values C_{dl} with the increase in inhibitor concentration is due to the increase in quantum of adsorption of inhibitor molecules on the corroding surface.
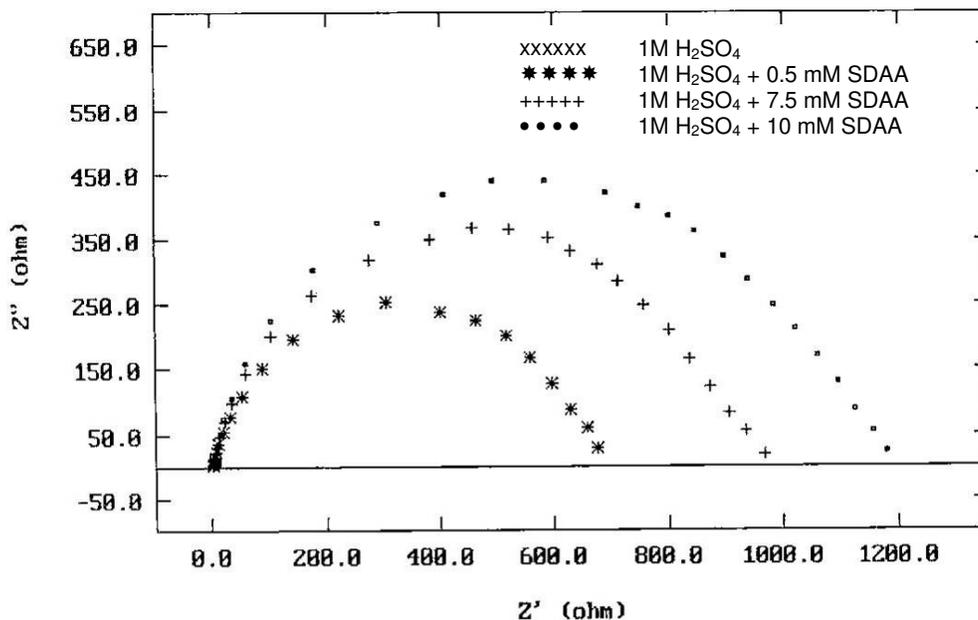
Figure 4. Nyquist diagram for mild steel in 1M sulphuric acid for selected concentrations of SDAA
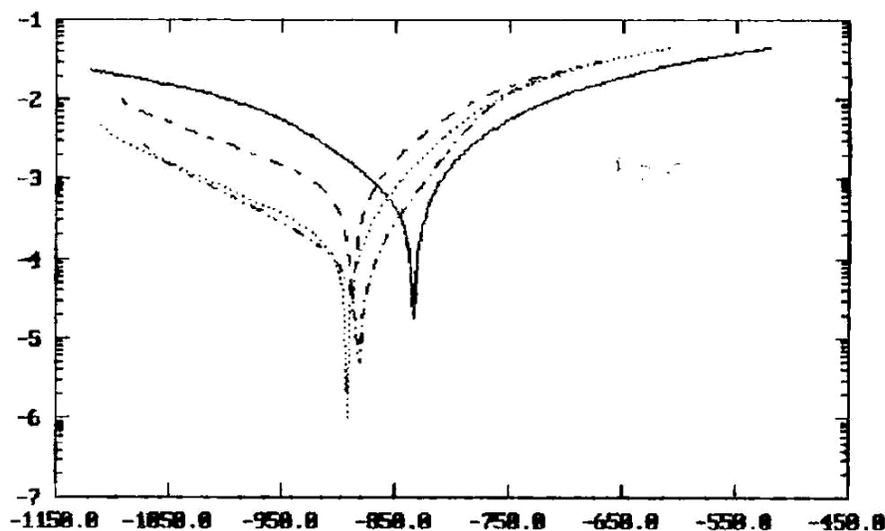
Figure 5. Polarization curves of mild steel recorded in 1M sulphuric acid for selected concentrations of SDAA

Table 6. Impedance method Impedance data of the inhibitors in 1M sulphuric acid at 30±1°C

Compound name	Inhibitor concentration (mM)	OCP (-) mV	C_{dl} µF/cm^2	R_t ohms/cm^2	Inhibition efficiency (%)
SDAA	Blank	438	23.08	8.93	-
	0.5	404	20.21	63.46	85.85
	7.5	478	4.30	98.49	90.93
	10	459	1.61	119.43	92.52
MDAA	Blank	438	23.08	8.93	-
	0.5	496	10.66	594.47	98.49
	7.5	490	1.627	619.48	98.55
	10	489	1.023	650.57	98.62
DAA	Blank	468.8	23.08	9.0524	-
	0.5	553.4	8.0853	81.2872	88.86
	7.5	529.4	4.418	851.53	98.96
	10	531.8	3.460	1022.57	99.11
ODAA	Blank	468.8	23.08	3.407	-
	0.5	553.4	16.9	9.91	65.62
	7.5	529.4	9.45	17.08	80.05
	10	531.8	2.64	38.30	91.10

1 Polished

2 Immersed in DAA in 1M sulphuric

3 Immersed in MDAA in 1M sulphuric

4 Immersed in SDAA in 1M sulphuric

5 Immersed in ODAA in 1M sulphuric

6 Immersed in 1M sulphuric acid
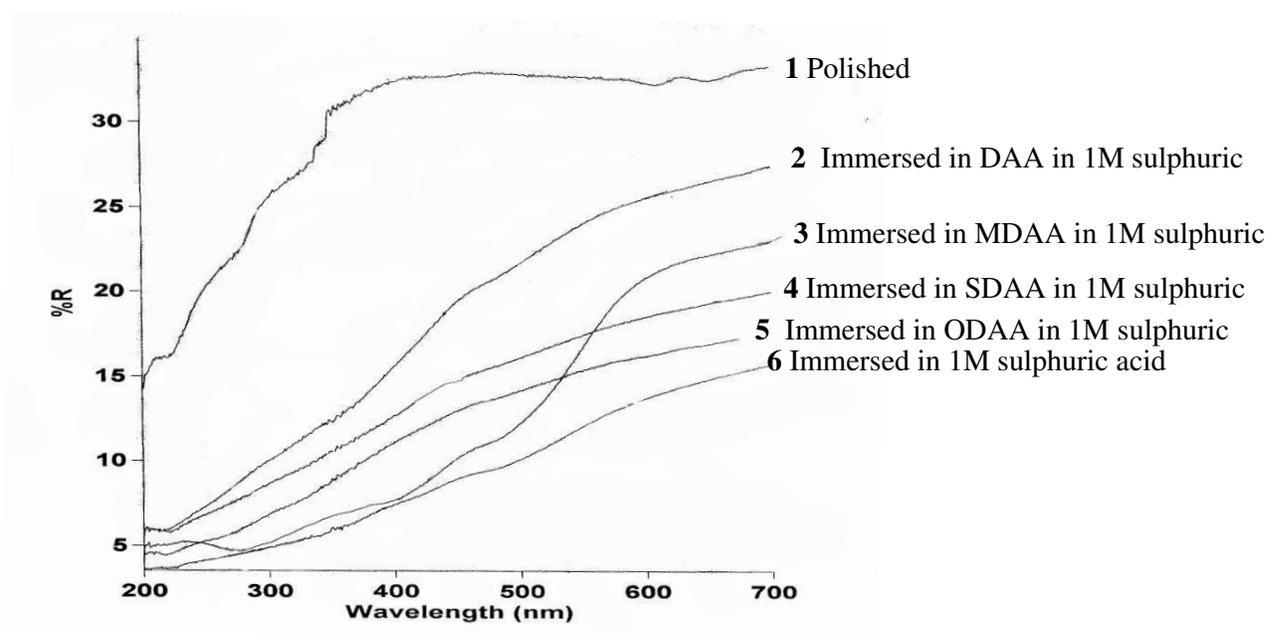
Figure 6. UV reflectance spectra of mild steel immersed in the presence and absence of inhibitors

Table 7. Polarization data of the inhibitors in 1M sulphuric acid at 30±1°C

Compound name	Inhibitor concentration (mM)	OCP (-)mV	b_a mV/dec	b_c mV/dec	E_{corr} (-)mV	I_{corr} $\mu A/cm^2$	Inhibition efficiency (%)
SDAA	Blank	401	76.92	126.92	443.07	1624	-
	0.5	488	50	115.38	480.77	630.95	61.14
	7.5	490	75	155	495.7	537.0	66.93
	10	479	50	111.53	505.4	142.5	91.23
MDAA	Blank	487.2	67.76	148.15	487.88	4467	-
	0.5	550.1	50.09	141.58	493.75	971.81	78.24
	7.5	528.7	47.20	124.02	489.16	365.11	91.82
	10	533.8	49.55	129.78	477.30	125.97	97.17
DAA	Blank	487.2	64.89	121.32	464.64	1571.0	-
	0.5	550.1	41.17	113.32	541.28	105.2	93.3
	7.5	528.7	39.43	121.70	527.49	14.62	99.06
	10	533.8	36.80	138.08	522.99	10.425	99.33
ODAA	Blank	401	76.92	126.92	473.07	1624	-
	0.5	437	50	88.46	437.97	774.46	52.31
	7.5	461	50	96.15	450.00	336.5	79.28
	10	439	57.69	96.15	432.5	184.9	88.61

3.4. Potentiodynamic polarization data

Potentiodynamic polarization experiments were performed at 30±1°C for mild steel in solutions containing 1M sulphuric acid and various concentrations of the four inhibitors DAA, MDAA, SDAA, ODAA ranging from 0.5 mM to 10 mM. The potentiodynamic polarization data derived from the plots (figure 5) are presented in table 7. The corrosion current density (I_{corr}) values were obtained by extrapolating both the cathodic and anodic Tafel slopes to the corrosion potential (E_{corr}). As both cathodic and anodic slopes namely b_c and b_a are altered by the addition of inhibitors, the inhibitors retard the cathodic hydrogen evolution and anodic metal dissolution.

4. DISCUSSION

For all the four inhibitors, the surface coverage increased with increases in concentration and reach a limiting value at higher inhibitor concentration. Correlation between θ values and inhibition

efficiency suggests that the inhibitive action is through adsorption. The negative free energy of adsorption infers that the inhibition is through spontaneous adsorption of inhibitors. (table 4)

4.1. Mechanism of adsorption of Schiff bases compounds on the metal surface.

Inhibitors MDAA, SDAA, DAA and ODAA contain four aromatic rings and two –CH = N– groups. These inhibitors may be adsorbed on the mild steel surface through a combination of the following three probable adsorption mechanisms (shown schematically below).

- Protonation of nitrogen atoms of –CH=N– group could make the inhibitor molecule positively charged. Iron surface gets negatively charged in sulphuric acid. This could lead to an interaction occurs between positively charged inhibitor molecule and negatively charged metal surface
- Unshared electron pairs on nitrogen atom could interact with metal surface.
- The flat orientation of the entire molecule with respect to the metal surface could lead to the interaction of π-electrons of the aromatic ring as well as –CH=N– Groups with the metal surface (c).
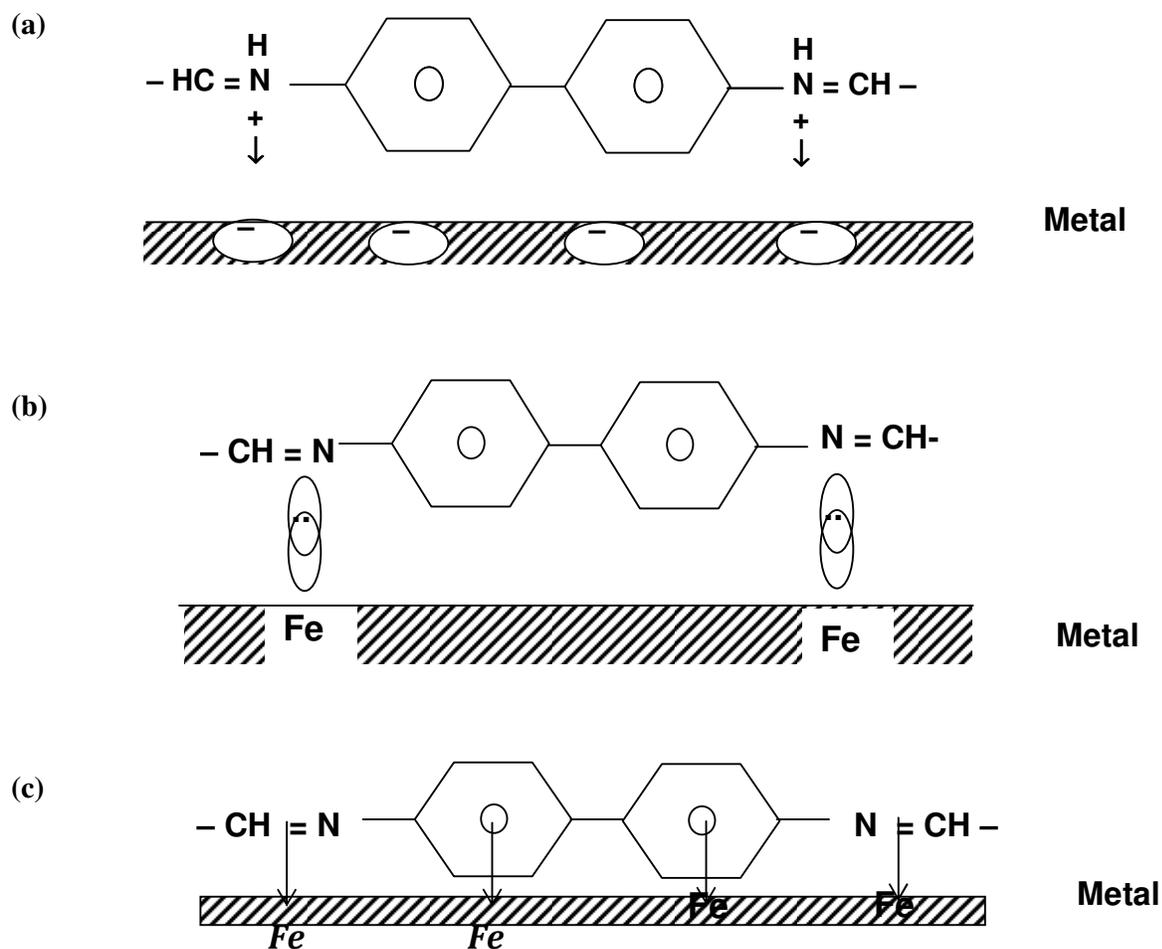
Scheme 3. Effect of introducing groups between phenyl rings of dianils on inhibition efficiency

Order of inhibition efficiency of four inhibitors is,

MDAA ≈ DAA > SDAA > ODAA
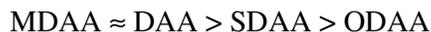
It is proposed that ODAA has lowest inhibition efficiency due to the introduction of electronegative oxygen atom between the biphenyl systems, which reduces the π-electron density of the two aromatic rings. MDAA & DAA have almost same inhibition efficiency indicating that introduction of a –CH$_2$– group in MDAA has not caused any appreciable change in inhibition efficiency. Inspite of the presence of comparatively less electronegative sulphur atom, inhibition efficiency of SDAA is marginally lower than the other two, obviously due to the existence of two highly electronegative oxygen atom on sulphur atom. The intervening groups obviously have not affected the general mechanisms of adsorption through the flat orientation of the molecule.

5. NATURE OF ADSORPTION AND THE EFFECT OF TEMPERATURE ON INHIBITION EFFICIENCY

Two types of adsorption may be distinguished i.e. physical and chemical. Of the 3 mechanisms proposed for adsorption, first mechanism is physical type and the remaining two are chemisorptions. In the present case, adsorption is thought to be a combination of physical and chemical adsorption as all the three adsorption mechanisms are involved. However which predominates over the other is detected from the temperature studies. Inhibition efficiency decreases with increase in temperature. Ea values for inhibited acids is higher (40 to 85 kJ/mole). $-\Delta G°_{ads} \approx 7$ to 16 kJ/mole. According to Radovici, physisorption predominates if inhibition efficiency decreases with increase in temperature. Hence, it can be concluded that in the adsorption of the Schiff bases, it is the physisorption which predominates. Furthermore, a plot of logθ/1-θ vs log C gives a straight line indicating Langmuir adsorption isotherm.

5.1. Impedance behavior of inhibition

The increase in charge transfer resistance (R_t) and decrease in double layer capacitance (C_{dl}) may be attributed to the increased adsorption of the inhibitors on the metal surface. The semicircular nature of the Nyquist plots indicates that the corrosion of steel is mainly controlled by charge transfer process. An electrode process may be diffusion controlled are activation controlled or by a contribution of both. If the corrosion process is purely diffusion controlled, the Nyquist plot will be a straight line with 45° slope. On the other hand, if the process is activation polarization controlled Nyquist plot will be semicircle with a radius of (R_t/2) as given in figure below.

5.2. Polarization behavior of inhibition

The inhibitors SDAA, MDAA, DAA and ODAA shifted both the anodic and cathodic Tafel polarization curves to an appreciable extent. The cathodic and anodic Tafel slopes viz., b_c and b_a were

also altered without any appreciable change in E_{corr} value except for DAA. DAA shifted the corrosion potential E_{corr} values slightly to the negative direction. Hence all the four inhibitors may be classified as mixed inhibitors in which DAA is slightly cathodic in nature.
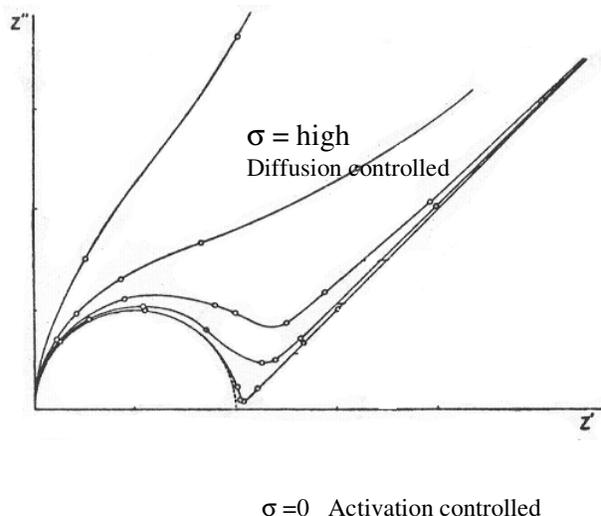
Scheme 4. Effect of change in σ on the Nyquist plots

For the present investigations all the Nyquist plots are semicircular in nature and hence all the inhibited systems in the current Chapter are activation controlled.

5.3. UV reflectance spectral studies

The fact that inhibition of corrosion of mild steel in acidic solutions in the presence of these Schiff organic compounds, may be due to the formation of a blanket of inhibitor on the metal surface, is also supported by reflectance studies carried out using a spectrophotometer for the same specimens under different conditions. The reflectance curves drawn on a uniform scale for polished mild steel specimens, mild steel specimens immersed in 1M sulphuric acid alone and in the presence of MDAA, SDAA, DAA and ODAA (10 mM) are shown in Figure VI. It can be seen from these curves that the percentage of reflectance is maximum for a polished specimen and it has been reduced considerably in the case of specimens immersed in plain 1M sulphuric acid. This observation clearly revealed the change in surface characteristics due to the corrosion of mild steel in plain 1M sulphuric acid. However in the case of specimens immersed in 1M sulphuric acid containing 10 mM concentration of MDAA, SDAA, DAA and ODAA reflectance has been reduced to only a very small extent. This shows that surface characteristics are not altered very much, due to the formation of a blanket of inhibitor on the surface. A close look at the UV reflectance spectra figure 6 clearly revealed the fact that the performance of DAA is best in this regard, followed by MDAA, SDAA and ODAA in the decreasing order.

5.4. SEM

The formation of an adsorbed protective film of the inhibitor molecule on the mild steel surface is also confirmed by SEM studies.
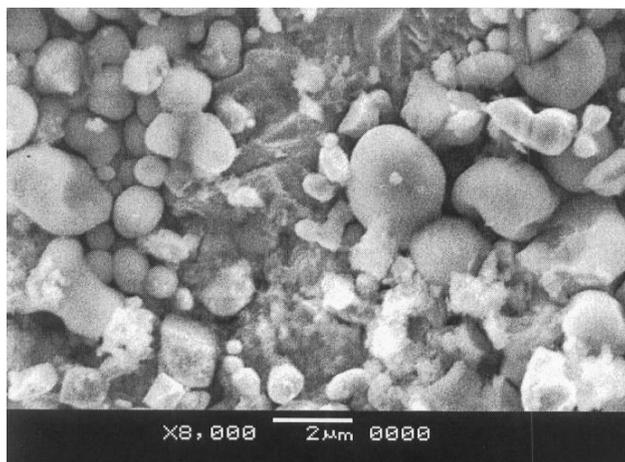
Figure 7. Sem photograph of mild steel immersed in 1M sulphuric acid

Figures 7 and 8 show scanning electron micrographs of mild steel specimens exposed to 1M sulphuric acid and 1M sulphuric acid containing 10 mM concentration of the inhibitor DAA. Uniform corrosion can be observed in figure 7. SEM obtained for blank indicates corrosion products with metal oxygen bonds (M-O) similar to those observed for metal hydroxides and oxides. However, the SEM obtained for inhibited mild steel specimen indicates that the metal surface is fully covered with inhibitor molecules giving it high degree of protection figure –8.
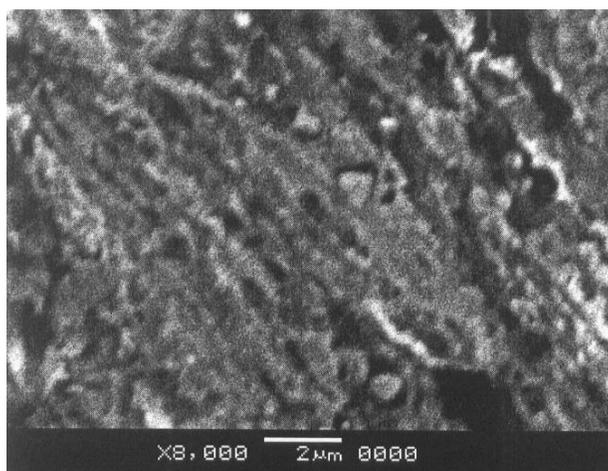
Figure 8. Sem photograph of mild steel immersed in 1M sulphuric acid containing 10 mM of DAA

5.5. Atomic absorption spectroscopy (AAS)

The amount of iron dissolved in the presence of SDAA, MDAA, DAA and ODAA when mild steel specimens were exposed to 1M sulphuric acid was calculated and the data are presented in table 8. It was found that the amount of dissolved iron in the corrodant solution decreased with increase in concentration of the inhibitor. There is good agreement between values of percentage inhibition efficiency calculated from weight loss and AAS technique.

Table 8. Amount of dissolved iron present in the corrosive solution (1M sulphuric acid) containing inhibitors by AAS

Name of the inhibitor	Inhibitor concentration (mM)	Amount of iron in corrodant (mg/l)	Inhibition efficiency (%)
	Blank	2792.8	-
MDAA	0.5	500.0	82.09
	5	135.6	95.14
	10	17.2	99.38
SDAA	0.5	203.75	92.70
	5	187.50	93.28
	10	120.0	95.70
DAA	0.5	367.0	86.83
	5	105.0	96.21
	10	14.9	99.46
ODAA	0.5	350.0	87.46
	5	280.0	89.97
	10	240.0	91.40

5.6. FTIR spectroscopy

The structures of the inhibitors were confirmed by FTIR spectroscopy. The FTIR spectra of MDAA, SDAA, DAA and ODAA. The characteristic peaks, 1598-1575 cm^{-1} (C=N stretching), 1620-1630 cm^{-1} (aromatic ring breathing vibrations), ~1070 cm^{-1}(C–N stretching), confirm the structures of the inhibitors. In addition, the presence of two bands at 1286.4 cm^{-1} and 1143 cm$^{-1,}$ is characteristic of S=O stretching and C –S stretching at 698.2 cm^{-1} confirm the structure of SDAA. ODAA displays a band at 1282 cm^{-1}, characteristic of = C– O stretching of ether grouping.

The FTIR spectra of the corrosion products show several modifications in the range 1595-1616 cm^{-1} (due to C =N and aromatic ring). FTIR spectra of the corrosion product obtained after immersion

in solution containing 1M H_2SO_4 and SDAA exhibit new bands around 2360 cm^{-1} and 2330 cm^{-1} characteristic of – S – H stretching. This may be attributed to the reduction of –SO_2 to –SH by the hydrogen evolved at the electrode surface for which iron acts as a catalyst. This is in accordance with the findings of Schwabe[29]. Similarly FTIR spectrum of corrosion product with ODAA shows new bands at 3766.7 cm^{-1} and 3415.7 cm^{-1} which is characteristic of O – H stretching vibration. The appearance of this band may probably be due to the reduction of C– O– C group to – C – OH by the hydrogen evolved at the surface of the electrode. Hence it can be concluded that the lower adsorbability of SDAA and ODAA may be due to their decomposition to – SH and – OH compounds which have a lesser tendency to adsorb on the metal surface[30,31].

6. Conclusions

- The dianiline Schiff bases act as efficient corrosion inhibitors in 1M sulphuric acid and they exhibit a maximum inhibition efficiency of 95-99 %. The dianiline Schiff bases inhibit corrosion of mild steel in the following order

  MDAA ≈ DAA > SDAA > ODAA
- No significant increase in inhibition efficiency is observed by the introduction of –O–, – SO_2– and –CH_2– atom/ groups between the two phenyl groups of DAA.
- The adsorption of all the four dianiline Schiff bases on a mild steel surface obeys the Langmuir adsorption isotherm.
- Inhibition efficiency of the dianiline Schiff bases decreases with increase in temperature and further it leads to an increase in activation energy.
- The less negative $\Delta G°_{ads}$ values suggest physisorption of the inhibitors on the metal surface.
- All the four dianiline Schiff bases influence both cathodic and anodic processes and hence behave as mixed type inhibitors except DAA which is slightly cathodic in nature.

  SEM photographs and UV reflectance spectra clearly reveals that there is a change in the surface characteristics of the metal surface due to the addition of the dianiline Schiff bases.

References

1. Mirghasem, Hosseini, Stijin, F.L. Mertens, Mohammed Ghorbani and Mohammed, R. Arshadi, *Mater. Chem. and Phy.,* 78 (2003) 800.
2. P.C. Okafor and E.E. Ebenso *Trans. SAEST.,* 38 (2003) 91.
3. S. Ellayyoubi and B. Hammouti *Trans. SAEST.,* 37 (2003) 29
4. M.A. Quraishi and Ranasardar, *Bull. Electrochem.,* 19 (2003) 209.
5. E.E. Ebenso, *Bull. Electrochem.,* 19 (2003) 209.
6. V.Violet Dhayabaran, T. Jeyaraj, C. Raja and N. Shobana, *Trans. SAEST.,* 38 (2003) 7.
7. J.T. Patel and B.N. Oza, *Trans. SAEST.,* 38 (2003) 37.
8. F.Bentiss, M. Traisnel and M. Lagrenee, *J. Appl. Electrochem.,* 31 (2001) 41.
9. K.Madhavan,S. Muralidharan, S. Venkatakrishna Iyer,*Bull.Electrochem.*17(2001)215.
10. S.Muralidharan, R. Chandrasekar and S.V.K. Iyer, *Proc. Indian Acad. Sci. Chem Sci.,* 112 (2000) 127.

11. M.N. Desai, M.B. Desai, C.B. Shah, S.M. Desai, *Corros. Sci.,* 26 (1986) 827.
12. H. Shokry, M. Yuasa, I. Sekina, R.M. Issa, H.Y.El. Baradie, G.K. Gomma, *Corros. Sci.,* 40 (1998) 2173.
13. G.K. Gomma, M.H. Wahdan, *Mater. Chem. Phy.,* 39 (1995) 209.
14. S.Li, S.Chen, S.Lei, H.Ma, R.Yu, D.Liu, *Corros. Sci.,* 41 (1995) 2173.
15. S.L.Li., Y.G. Wang, S.H. Chen, R.Yu, S.B. Lei, H.Y. Ma, D.X. Liu.,*Corros. Sci.,* 41 (1991) 1769.
16. Z.Quan, S.Chan, Y.Li, X.Lui, *Corros. Sci.,* 44 (2002) 703.
17. H.Ma, S.Chen, L. Niu, S. Shang, S.Li, S. Zhno, Z. Quan,*J. Electrochem. Soc.,* 148 (2001) 132.
18. T.Vasudevan,S.Muralidharan,S. Alwarappan, S.V.K. Iyer, *Corros. Sci.,*37 (1995) 1235.
19. G.Schmitt,*Br. Corros. J.,* 19 (1984) 165.
20. E.C.Turibina, E.E.Berdikhina,V.V.Pikuler,T.R.Chelyabinok,*Politech Inst.,*91 (1971) 16.
21. S.Muralidharan, M.A. Quraishi and S.V.K.Iyer, *Corros. Sci.,* 37 (1995) 1794.
22. M.A. Quraishi, M.A. Wajidkhan, M. Ajmal, S.Muralidharan and S.V.K. Iyer., *Br. Corros. J.,* 32 (1997) 72.
23. S.Bilgic, N. Cabiskan, *J. Appl. Electrochem.,* 31 (2001) 79.
24. D.F. Shirver, P.W. Attinz, C.H. Langford, *Inorg. Chem.* 2*nd Edn. Oxford Univ. Press*. Oxford, 239.
25. T.Tsuru, S. Haruyama and B. Gijustsu, *J. Jpn. Soc. Corros. Eng.,* 27 (1978) 27.
26. J.E.B.Randles, *Disc. Faraday Soc.,* 1 (1947) 11.
27. P.Delahay, *J. Phy. Chem.,* 70 (1996) 2373.
28. J.H. Sluyters, *RECUEIL,* 79 (1960) 1092.
29. K.Schwabe, *Z. Phys. Chem.,* 1 (1964) 226.
30. V.S. Komkhadze and S.A. Balezin, *Zh. Obshch. Khim.,* 22 (1952) 1848.
31. G.P. Cicileo, B.M. Rosales, F.E. Vavela and J.R. Vilche, *Corros. Sci.*, 41(1999) 1359.